



Effects of Aneuploidy on Cellular Physiology and Cell Division in Haploid Yeast

Eduardo M. Torres, *et al.*

Science **317**, 916 (2007);

DOI: 10.1126/science.1142210

The following resources related to this article are available online at www.sciencemag.org (this information is current as of August 23, 2007):

Updated information and services, including high-resolution figures, can be found in the online version of this article at:

<http://www.sciencemag.org/cgi/content/full/317/5840/916>

Supporting Online Material can be found at:

<http://www.sciencemag.org/cgi/content/full/317/5840/916/DC1>

A list of selected additional articles on the Science Web sites **related to this article** can be found at:

<http://www.sciencemag.org/cgi/content/full/317/5840/916#related-content>

This article **cites 29 articles**, 10 of which can be accessed for free:

<http://www.sciencemag.org/cgi/content/full/317/5840/916#otherarticles>

This article appears in the following **subject collections**:

Cell Biology

http://www.sciencemag.org/cgi/collection/cell_biol

Information about obtaining **reprints** of this article or about obtaining **permission to reproduce this article** in whole or in part can be found at:

<http://www.sciencemag.org/about/permissions.dtl>

Effects of Aneuploidy on Cellular Physiology and Cell Division in Haploid Yeast

Eduardo M. Torres,¹ Tanya Sokolsky,^{1*} Cheryl M. Tucker,² Leon Y. Chan,¹ Monica Boselli,¹ Maitreya J. Dunham,² Angelika Amon^{1†}

Aneuploidy is a condition frequently found in tumor cells, but its effect on cellular physiology is not known. We have characterized one aspect of aneuploidy: the gain of extra chromosomes. We created a collection of haploid yeast strains that each bear an extra copy of one or more of almost all of the yeast chromosomes. Their characterization revealed that aneuploid strains share a number of phenotypes, including defects in cell cycle progression, increased glucose uptake, and increased sensitivity to conditions interfering with protein synthesis and protein folding. These phenotypes were observed only in strains carrying additional yeast genes, which indicates that they reflect the consequences of additional protein production as well as the resulting imbalances in cellular protein composition. We conclude that aneuploidy causes not only a proliferative disadvantage but also a set of phenotypes that is independent of the identity of the individual extra chromosomes.

The cell division cycle is a highly controlled process that generates two daughter cells of identical genetic makeup. Surveillance mechanisms known as checkpoints ensure that this process occurs with high fidelity. However, despite these surveillance mechanisms, chromosome missegregation occurs once every 5×10^5 cell divisions in yeast (1) and on the order of once every 10^4 to 10^5 divisions in mammalian cells (2), producing a condition known as aneuploidy.

More than a century ago, aneuploidy was postulated to be a common characteristic of cancer cells (3). Since then, it has been proposed that aneuploidy contributes to tumorigenesis by providing a mechanism by which oncogenes are gained or tumor suppressor genes are lost (4). Studies examining the effects of aneuploidy on cell proliferation in *Schizosaccharomyces pombe* (5) and *Drosophila* (6) and the effects of trisomy on cell proliferation in humans (7) suggest that aneuploidy can also interfere with cell proliferation. To address how aneuploidy affects the proliferation and physiology of normal cells, we generated a set of yeast strains in which each strain bears an extra copy of one or more of almost all of the yeast chromosomes. Their characterization represents a comprehensive analysis of the effects of aneuploidy on cellular physiology. We found that in addition to chromosome-specific phenotypes, aneuploid strains share a

number of traits, pointing toward the existence of a general cellular response to aneuploidy.

Generation of aneuploid yeast strains. To create yeast cells that contain an additional chromosome, we used a chromosome transfer strategy. During mating, if one of the mating partners lacks the karyogamy gene *KAR1*, nuclear fusion does not occur (8). However, occasionally individual chromosomes are transferred from one nucleus to the other during these abortive matings (8, 9). When the two mating partners carry different selectable markers at the same genomic location, these rare chromosome transfers can be selected for (fig. S1). Using this technique, we generated 13 of the 16 possible disomic strains (tables S1 and S2) (10).

To ensure that strains with the correct marker combination were indeed disomic for the entire chromosome, we performed comparative genomic hybridization, which allows for the quantification of gene copy number on a genome-wide scale. This analysis also revealed that some of the strains obtained from the chromosome transfer procedure carried one or two extra chromosomes in addition to the one we selected for (fig. S2A). Although the second chromosome cannot be selected for, these strains were karyotypically stable enough to conduct a phenotypic characterization.

Aneuploidy causes a transcriptional response. To characterize the effects of aneuploidy on gene expression, we grew each aneuploid yeast strain to mid-log phase in batch culture and measured genome-wide gene expression relative to the wild-type strain with the use of DNA microarrays. An approximate doubling of gene expression was observed along the entire length of the disomic chromosomes, indicating that most if not all genes are expressed proportionally to the number of DNA copies in the cell

(Fig. 1A). A similar result has been reported for a smaller data set (11).

To reveal more subtle correlations masked by the strong chromosome-specific signals (fig. S3A), we applied a clustering program that allows the assignment of a reduced weight to genes on disomic chromosomes (10) (Fig. 1B). This analysis showed that many aneuploid yeast strains—particularly strains disomic for chromosomes IV, XIII, XV, and XVI and strains with multiple extra chromosomes—exhibited a gene expression signature characteristic of the yeast environmental stress response (ESR). Of the 870 genes identified by Gasch *et al.* to constitute the ESR cluster, 615 also showed the same transcriptional change in yeast strains with additional chromosomes (Fig. 1B) (12). These same expression changes are also observed in yeast strains growing at slower growth rates (13). Mutants defective in cell proliferation, such as temperature-sensitive *cdc28-4* or *cdc23-1* grown at the permissive temperature (*cdc28-4* mutants exhibit a G₁ delay; *cdc23-1* mutants exhibit a metaphase delay), also exhibited some of the same changes in gene expression (Fig. 1B), raising the possibility that defects in cell proliferation could also cause this transcriptional response.

All aneuploid strains that we examined proliferated more slowly than did wild-type cells (fig. S4, A, B, F, and G). Gene expression patterns that are linked to growth rates could thus mask gene expression patterns common to all aneuploid strains. To eliminate differences in gene expression caused by differences in doubling time, we grew all aneuploid strains and the wild type at the same growth rate in the chemostat under conditions where phosphate was limiting. Because the set doubling time of ~6 hours was longer than the doubling time of each strain in batch growth, all strains grew at the same rate. When cells reached steady state, samples for gene expression were harvested for microarray analysis. Slow-growing strains carrying the *cdc28-4* and *cdc23-1* mutations were also grown under the same conditions. The gene expression changes that correlated with growth rate differences were not present in any of the chemostat-grown samples. The remaining gene expression changes included a transcription pattern shared by most of the aneuploid strains and not detectable or not present in exponentially growing cultures, nor in wild-type cells or *cdc28-4* and *cdc23-1* mutants grown in the chemostat under phosphate-limiting conditions (Fig. 1C and fig. S3B).

Of the 4963 genes whose expression change was greater than the control threshold (factor of 1.3) in at least one strain, 397 genes showed changed expression in 10 or more of the 14 aneuploid strains. We used the program GO Term Finder, available from the *Saccharomyces* Genome Database (14), to identify the functional categories enriched in each gene set. The group that showed increased expression was enriched

¹Center for Cancer Research, Howard Hughes Medical Institute, Massachusetts Institute of Technology, E17-233, 40 Ames Street, Cambridge, MA 02139, USA. ²Lewis-Sigler Institute for Integrative Genomics, Princeton University, Princeton, NJ 08544, USA.

*Present address: Applied Biosystems, 500 Cummings Center, Beverly, MA 01915, USA.

†To whom correspondence should be addressed. E-mail: angelika@mit.edu

in ribosomal biogenesis genes, particularly those related to ribosomal RNA processing (Fig. 1D and table S4). Genes with annotations related to nucleic acid metabolism were also enriched (table S4). The more variable set of genes whose expression was decreased was enriched for genes involved in carbohydrate metabolism (Fig. 1D and table S4). We conclude that aneuploid strains, when normalized for growth rate in phosphate-limited chemostats, are somehow perturbed with respect to ribosomal biogenesis and energy production.

Most aneuploid yeast strains exhibit a G₁ delay. To determine how aneuploidy affects cell physiology, we characterized the proliferation properties of strains carrying one or several extra chromosomes. The doubling time and cell size were slightly increased in most aneuploid strains in complete medium [yeast extract, peptone, and dextrose (YPD); fig. S4A] and synthetic medium that selects for the presence of the disome (-His+G418; fig. S4B). Even disomic strains that did not exhibit a proliferation delay, such as cells disomic for chromosomes I or II, showed decreased proliferative capacity relative to wild-type cells when the strains were cocultured (fig. S4, F and G). Furthermore, some of the aneuploids, such as strains disomic for chromosomes IV, XI, or XIII, also exhibited poor viability as judged by their inability to form colonies on plates (fig. S4E). The proliferative disadvantage and increase in cell size were also observed in diploid cells carrying an extra chromosome (fig. S4, C and D), indicating that the gain of an extra chromosome interferes with cell proliferation of both haploid and diploid cells. Thus, contrary to what we would have expected from studies on cancer cells, where aneuploidy is thought to bring about a proliferative advantage (4), aneuploidy causes a proliferative disadvantage in yeast.

To determine in which stage of the cell cycle the aneuploid yeast strains were delayed, we examined cell cycle progression after release from a pheromone-induced G₁ phase arrest. Entry into the cell cycle, as judged by bud formation (Fig. 2A) and DNA replication (Fig. 2B), was delayed in 16 of 20 aneuploid strains. With the exception of cells disomic for chromosomes I, II, V, or IX, all aneuploid strains exhibited a delay in entry into the cell cycle (fig. S5 and table S1), with most strains (disome VIII, X, XI, XII, XIII, XIV, V+IX, VIII+XV, and XI+XV strains) showing a delay ranging from 10 to 20 min. Cells disomic for multiple chromosomes (disome V+VII, VIII+XIV, XI+XVI, and I+VI+XIII strains), as well as cells disomic for chromosome IV or XVI, exhibited a G₁ delay of 25 min or more. Aneuploids exhibited few other cell cycle delays. The metaphase to anaphase transition was delayed in only 2 of the 20 aneuploid strains (fig. S5 and table S1), and only 7 of 20 exhibited a delay in entry into mitosis (as determined by a delayed appearance of cells with metaphase spindles) (Fig. 2C, table S1, and fig. S5). We conclude that most aneuploid strains are delayed

in G₁ phase. In general, the delay appears to be larger in strains carrying an extra copy of a large chromosome or extra copies of multiple chromosomes (fig. S6), which suggests that the amount of additional yeast DNA may contribute to determining the length of the G₁ delay.

The molecular events underlying the G₁ to S phase transition are well characterized in *S. cerevisiae*. The cyclin-dependent kinase (CDK) Cdc28 associated with the cyclin Cln3 inhibits Whi5, an inhibitor of the transcription factor complex SBF (15, 16). SBF in turn induces the transcription of genes encoding two other cyclins, *CLN1* and *CLN2*, which, when complexed with Cdc28, promote entry into the cell cycle (17). We analyzed the abundance of *CLN2* RNA and Cln2 protein in strains disomic for chromosomes IV, XIII, or VIII+XIV. Accumulation of *CLN2* RNA and Cln2 protein was delayed and paralleled the delay in bud formation and DNA replication (Fig. 2, D and E). Our results indicate that in the strains that we analyzed, aneuploidy interferes with the G₁ to S phase transition upstream of *CLN2* transcription. How the presence of additional yeast chromosomes prevents Cln2 accumulation remains to be determined. Cln3-CDKs promote *CLN2* accumulation and are the target of events such as cell growth that control the G₁ to S phase transition (18, 19). Thus, the presence of extra chromosomes might affect Cln3-CDK function.

Aneuploids exhibit increased glucose uptake. To further investigate the effects of aneuploidy on cell proliferation, we examined the kinetics with which aneuploid cells enter stationary phase. Most aneuploids reached saturation at a smaller population size [as measured by optical density at 600 nm (OD₆₀₀)] (Fig. 3, A and B) and lost viability upon prolonged culturing in stationary phase (Fig. 3C). In general, the maximum OD₆₀₀ was lower in strains carrying two copies of large chromosomes or two copies of multiple chromosomes (Fig. 3, A and B). Thus, biomass accumulation appears to be inversely correlated with the amount of additional yeast DNA present in the aneuploid strains and the severity of their proliferation defects.

To determine whether the lower OD₆₀₀ at which aneuploids enter stationary phase was due to nutrient depletion, we simultaneously measured glucose uptake and accumulation of biomass. This comparison revealed that wild-type cells generated more biomass per internalized glucose molecule than did aneuploid cells. Whereas wild-type cells reached cell densities of OD₆₀₀ = 9, having taken up 75% of the glucose in the medium, cells disomic for chromosome IV only reached a cell density of OD₆₀₀ of less than 4 (Fig. 3D). The increase in glucose uptake correlated with the severity of the cell cycle delay, with strains with a shorter doubling time accumulating more biomass per glucose molecule (Fig. 3E).

Consistent with the idea that aneuploids take up more glucose, we observed that the gene loci

encoding the high-affinity glucose transporters Hxt6 and Hxt7 were amplified (fig. S2B) and more highly expressed (Fig. 1 and fig. S2B) in most of the aneuploid strains we generated ($n = 42$). Strains that did not show this amplification and increased expression were those that carried an extra copy of chromosome VIII, which carries three genes encoding other high-affinity glucose transporters. Together with the microarray experiments indicating changes in gene expression relating to carbohydrate metabolism, our results suggest that aneuploids require more carbohydrates or energy (or both) for cell survival and proliferation than do wild-type cells.

Most genes on the aneuploids' extra chromosomes are expressed. Why would aneuploids need additional glucose? Because an estimated 60 to 90% of the intracellular chemical energy is devoted to protein production (20), we hypothesized that macromolecule biosynthesis from the additional chromosome present in aneuploid strains could be one reason. Indeed, our expression profile analysis of aneuploids showed that most genes present on the additional chromosomes were transcribed: 93% of genes carried on the chromosome that was present in two copies were overexpressed by a factor of at least 1.3 over the wild type, and expression of 83% of genes went up by a factor of 1.5 or more (Fig. 1, A and C). To determine whether the transcripts produced from the extra chromosomes were also translated, we measured the amounts of a small number of proteins. The amounts of Arp5, Tcp1, and Cdc28 protein were increased in strains disomic for the chromosomes containing the genes encoding these proteins (Fig. 4A). Our results suggest that at least some of the genes present on the additional chromosomes are not only transcribed but also translated.

Interestingly, most of the proteins (13 of 16) that we analyzed showed no change in abundance, even though the amount of transcript was increased in accordance with the increase in gene copy number (Fig. 4A and fig. S7). With the exception of Lcb4 and Fcy1 (for which it is not known whether they are components of protein complexes), all 13 proteins analyzed are components of protein complexes. Rpa1 is a component of the replication machinery, Mre11 of the RMX complex, Rps2 and Rpl32 of the ribosome, Rpt1 of the proteasome, Nop1 of the nucleolus, histone H3 of the nucleosome, Yaf9 and Eaf3 of the NuA4 histone H4 acetyltransferase complex, and Elp3 of the elongator complex. These findings indicate that many proteins synthesized from the additional chromosomes are either not translated or, more likely, degraded shortly after synthesis (21).

Consistent with the idea that increased protein degradation occurs in aneuploid yeast strains, the proliferation of a number of aneuploid strains (IV, XII, XIII, XIV, and XVI) was inhibited by concentrations of the proteasome inhibitor MG132 at which wild-type cells grow, as judged by their ability to form colonies on plates containing the

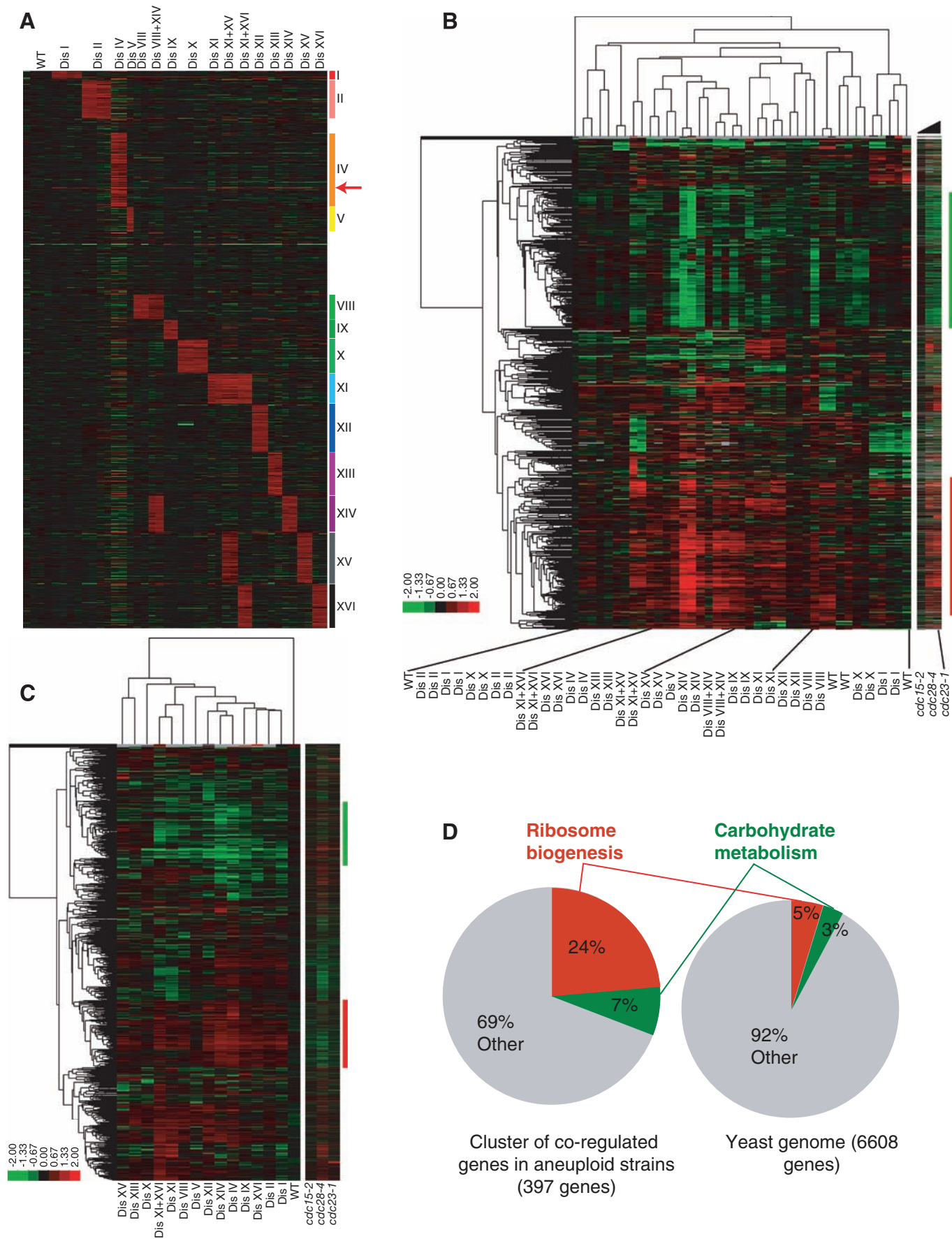


Fig. 1. Effects of aneuploidy on gene expression. **(A)** Gene expression of wild-type and aneuploid strains grown in batch cultures, ordered by chromosome position. Experiments (columns) are ordered by the number of the chromosome that is present in two copies. The expression patterns of aneuploid strains were compared to those of wild-type cells (A11311) grown under the same conditions. Data were renormalized to account for the disome. The arrow points to the genomic location of *HXT6* and *HXT7*. The data are provided in table S5. Strain order [note that the number after each strain number denotes the experiment number; the same nomenclature is used in (B)]: A11311 #1, A11311 #2, A11311 #3, A11311 #4, A12683 #1, A12683 #2, A6863 #1, A6863 #2, A12685 #1, A12685 #2, A6865 #1, A6865 #2, A12687 #1, A12687 #2, A14479 #1, A13628 #1, A13628 #2, A15615 #1, A15615 #2, A13975 #1, A13975 #2, A12689 #1, A12689 #2, A6869 #1, A6869 #2, A13771 #1, A13771 #2, A12691 #1, A12691 #2, A12699 #1, A12699 #2, A12693 #1, A12693 #2, A12695 #1, A12695 #2, A13979 #1, A13979 #2, A12697 #1, A12697 #2, A12700 #1, A12700 #2. **(B)** Hierarchically clustered gene expression data obtained from strains grown in batch cultures. Data from (A) were filtered for genes changing by a factor of >1.8 on at least two arrays. Genes present on chromosomes in two copies were downweighted and all data were clustered using the program WCluster. Clustering with all genes weighted equally is shown in fig. S3A. Gene expression for strains, ordered by increasing doubling time, carrying a *cdc15-2*, *cdc28-4*, or *cdc23-1* mutation compared to a matched wild type (A2587) grown at 23°C is shown adjacent to the main cluster. The columns labeled WT are biological replicates. Note that *cdc15-2* mutants do not show the ESR expression profile, which is consistent with the fact that *cdc15-2* mutants show only a slight proliferation defect at 23°C. Green and red bars correspond to putative clusters associated with ESR or growth rate that are down- and up-regulated, respectively. Replicates for each strain were more related to each other than to any other strains, indicating that the expression arrays were highly reproducible. Strain order: A11311 #4, A12685 #2, A12685 #1, A12683 #2, A12683 #1, A12689 #2, A12689 #1, A6865 #2, A6865 #1, A12699 #2, A12699 #1, A12700 #2, A12700 #1, A12687 #2, A12687 #1, A12695 #2, A12695 #1, A12691 #2, A12691 #1, A12697 #2, A12697 #1, A14479 #1, A13979 #2, A13979 #1, A15615 #2, A15615 #1, A13975 #2, A13975 #1, A13771 #2, A13771 #1, A12693 #2, A12693 #1, A13628 #2, A13628 #1, A11311 #3, A11311 #2, A6869 #2, A6869 #1, A6863 #2, A6863 #1, A11311 #1, A2596, A2594, A755. **(C)** Hierarchically clustered gene expression data obtained from strains grown in a chemostat under phosphate-limiting conditions. The expression patterns of aneuploid strains were compared to wild-type cells (A11311) grown under the same conditions. Data were renormalized, filtered for genes changing by at least a factor of 1.3 in at least one experiment, and clustered with genes present on chromosomes present in two copies downweighted. Clustering with all genes weighted equally is shown in fig. S3B. Gene expression for strains carrying a *cdc15-2* (A2596), *cdc28-4* (A2594), or *cdc23-1* (A755) mutation as compared to a matched wild type (A2587) grown at 23°C is shown adjacent to the main cluster. Green and red bars indicate putative common transcriptional responses that are down- and up-regulated in aneuploid strains, respectively. The data are provided in table S5. Strain order: A12697, A12695, A12689, A12699, A13771, A13628, A14479, A12693, A13979, A12687, A13975, A12700, A12685, A12683, A11311, A2596, A2594, A755. **(D)** Pie-chart representation of genes changing expression significantly in at least 10 of 14 disomic strains grown under phosphate-limiting conditions grouped by GO terms. Full GO results, including genes annotated to each term, can be found in table S4.

drug (Fig. 4F; note that strains with multiple additional chromosomes could not be tested because of the need to delete *PDR5* to test the effects of MG132) (22, 23). Furthermore, proliferation of all aneuploid strains was hampered by the protein synthesis inhibitor cycloheximide (Fig. 4C), which can be a sign of ubiquitin depletion (24). Several proteins such as α -tubulin and histones, which are components of multiprotein complexes, are degraded if they are overexpressed or their binding partners are missing (25, 26). Such a mechanism might regulate the amounts of the proteins that did not increase in abundance, in accordance with gene dosage in the aneuploid strains. Thus, transcription, translation, and degradation of proteins produced from the additional chromosomes present in aneuploids may contribute to the increased glucose uptake of these cells.

Proliferation of aneuploids is inhibited by protein synthesis inhibitors and high temperature. To determine whether the synthesis of proteins from the additional chromosomes and their presence in the cell represents an increased burden on the cell's protein production machin-

ery, we examined the ability of aneuploid strains to grow under conditions that interfere with transcription, protein synthesis, and protein folding. Proliferation of all aneuploids, with the exception of strains disomic for chromosomes I, X, or XIV, was inhibited by a high (20 $\mu\text{g/ml}$) concentration of the RNA polymerase inhibitor thiolutin (Fig. 4B). At low concentrations of the RNA polymerase inhibitor (5 $\mu\text{g/ml}$ to 15 $\mu\text{g/ml}$), proliferation of only a subset of strains was impaired (fig. S8H). However, all aneuploid strains showed decreased proliferation when exposed to the protein synthesis inhibitor cycloheximide at concentrations of 0.1 and 0.2 $\mu\text{g/ml}$, and proliferation of most strains was impaired at a concentration of 0.05 $\mu\text{g/ml}$ (Fig. 4C). With the exception of strains disomic for chromosomes I, II, or IX, aneuploid strains also showed increased sensitivity to the protein synthesis inhibitors hygromycin and rapamycin (Fig. 4D); cells disomic for chromosome X were not sensitive to rapamycin, perhaps because *TORI* is located on this chromosome). The proliferation-inhibitory effects of protein synthesis inhibitors on aneuploids was not a consequence of the proliferation defect of

aneuploids, because *cdc28-4* and *cdc23-1* mutants, which are severely impaired in cell division even at 23°C, did not exhibit increased sensitivity to cycloheximide or rapamycin (Fig. 4, C and D).

Proliferation of aneuploids was also decreased under conditions that led to the accumulation of unfolded proteins. All strains carrying an extra chromosome, with the exception of cells disomic for chromosome I, showed impaired proliferation at increased temperatures (37°C; Fig. 4E) and were modestly sensitive to the Hsp90 inhibitor geldanamycin (except cells disomic for chromosome X; Fig. 4F).

Aneuploids did not exhibit increased sensitivity to any toxic agents. Aneuploids formed colonies as well as did wild-type cells on medium containing the DNA replication inhibitor hydroxyurea (fig. S8B) or medium containing the proline analog azetidine 2-carboxylic acid (AZC; fig. S8E) or 6-azauracil (AZA; fig. S8I), which interferes with uridine triphosphate and guanosine triphosphate biosynthesis. None of the aneuploids showed altered proliferation in the presence of the autophagy inhibitor chloroquine (fig. S8D) or hydrogen peroxide (fig. S8G). Strains were also respiration-proficient as judged by their ability to grow on the nonfermentable carbon source glycerol (fig. S8, C and I) and did not exhibit increased sensitivity to the F1F0 adenosine triphosphate synthase inhibitor oligomycin (fig. S8I). About half of the aneuploid strains analyzed exhibited increased sensitivity to the microtubule-depolymerizing drug benomyl (fig. S8F), the basis of which warrants further investigation. Our results indicate that the proliferation of aneuploid strains is specifically impaired under conditions interfering with transcription, translation, and protein folding.

The phenotypes shared by aneuploid yeast strains are due to the presence of additional yeast genes. The phenotypes shared by aneuploids might result from the mere presence of additional DNA or from the RNAs and proteins synthesized from these chromosomes. Thus, we tested the effects of seven yeast artificial chromosomes (YACs) containing human or mouse DNA inserts ranging from ~350 kb to 1.6 Mb in size (table S3). Although we cannot exclude the possibility that some transcription and translation occurs from the mammalian DNA in yeast, the YACs do not produce yeast proteins, and it is highly likely that the amount of transcription and translation from the YACs is less than that occurring from yeast chromosomes, which are densely packed with mostly intronless genes.

The gene expression profile shared by aneuploid strains grown under phosphate-limiting chemostat conditions was also observed in YAC-carrying strains (Fig. 5A), which suggests that the mere presence of extra DNA is mainly responsible for this gene expression pattern. The other phenotypes observed in aneuploids were not shared by the YAC-bearing strains. With the exception of a minor (5 min) delay observed in cells carrying the largest YAC (YAC-1; 1.6 Mb),

none of the YAC-bearing strains exhibited delays in entry into the cell cycle (Fig. 5C). Nor was progression through other cell cycle stages affected, as judged by DNA content analysis (Fig. 5D). Furthermore, YAC-bearing strains did not exhibit increased sensitivity to thiolutin, cycloheximide, rapamycin, or high temperature (Fig. 5B). Curiously, the strain bearing the largest YAC exhibited increased sensitivity to hygromycin, the basis of which is at present unclear. We conclude that at least two aspects of aneuploidy may contribute to the phenotypes shared by aneuploid strains: (i) The expression signature shared by aneuploid strains appears to be elicited by the presence of extra DNA, and (ii) the cell cycle delays and proliferation defects under conditions interfering with protein synthesis and folding are in large part due to yeast transcripts and yeast proteins generated from extra chromosomes.

Discussion. Our analysis of aneuploid yeast strains was, by virtue of the way they were isolated, limited to aneuploid strains that are viable. Thus, most strains we characterized contained one additional chromosome, a few carried two, and one carried three. Strains with many additional chromosomes were not obtained, likely because they are inviable. The characterization of the 20 viable aneuploids that we analyzed nonetheless revealed that in addition to phenotypes that are chromosome-specific (for example, several aneuploid strains exhibit cell cycle defects in addition to the G₁ delay observed in most strains), these strains share several phenotypes.

Diploid yeast cells do not exhibit the phenotypes shared by the aneuploid strains we analyzed (figs. S4 and S8A). This result shows that the duplication of the entire genome is not nearly as deleterious as the duplication of a subset of chromosomes; moreover, it indicates that the genomic imbalance that results from aneuploidy is responsible for the phenotypes we observed. The finding that the severity of the phenotypes shared by aneuploids is generally greater in strains disomic for large or multiple chromosomes supports this idea. Our data further suggest that an increase in ploidy buffers the detrimental effects of the imbalances caused by aneuploidy. The phenotypes shared by aneuploids were generally less severe in trisomic than in disomic cells.

Our analysis of strains carrying YACs with mammalian DNA inserts suggests that most phenotypes common to aneuploids are caused by the additional yeast gene products. Only the gene expression pattern of aneuploids observed under phosphate-limiting conditions is also seen in the YAC-carrying strains, which suggests that the mere presence of extra DNA elicits this gene expression response. The cell cycle delay and impaired proliferation in the presence of transcription antagonists, translation inhibitors, or high temperatures were not observed in YAC-bearing strains. Most of the phenotypes shared by aneuploids—such as the increase in glucose uptake, the gene expression pattern observed in

logarithmically growing cells, impaired proliferation in the presence of proteasome inhibitors, and G₁ delay—appear to correlate with the number of additional yeast genes. In the case of other phenotypes, such as increased sensitivity to protein synthesis inhibitors and conditions requiring increased protein folding activity, the correla-

tion is not as striking. These findings, together with the observation that disomy for the small chromosome VI is lethal (10), indicate that the total amount of additional RNA and protein produced by aneuploids, the cellular imbalances caused by these extra proteins, and specific gene products present on individual chromosomes all

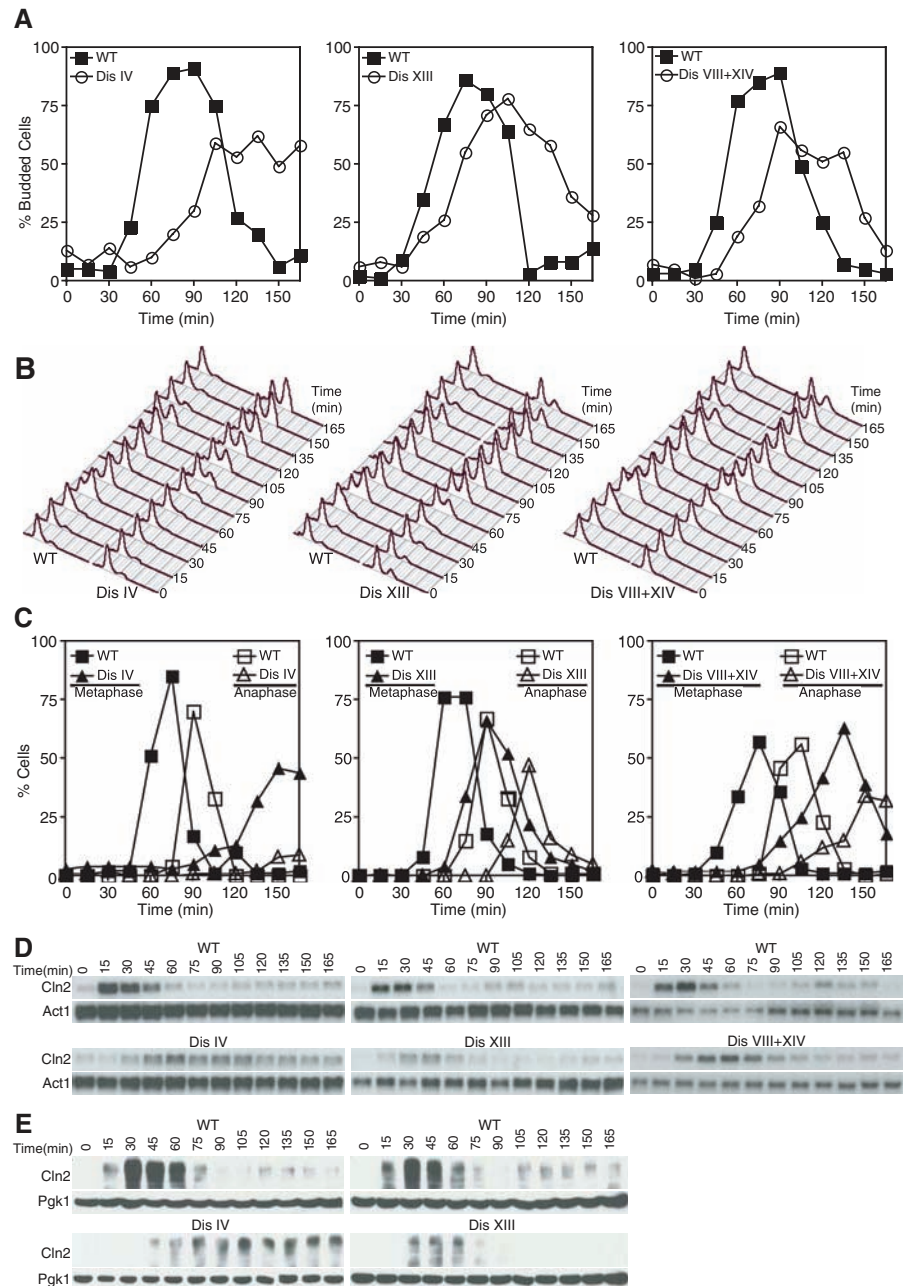


Fig. 2. Delay in G₁ of the cell cycle in aneuploid cells. Wild-type cells (A11311), cells disomic for chromosome IV (A12687), disomic for chromosome XIII (A12695), and disomic for chromosomes VIII and XIV (A15615), all carrying a *CLN2-HA* fusion with the exception of strain A15615, were arrested in G₁ with α -factor pheromone and released from the block as described (10). Samples were taken at indicated times to determine the percentage of budded cells (A), DNA content (B), the percentage of cells with metaphase and anaphase spindles (C), and the amount of *CLN2* RNA (D) and Cln2 protein (E). *ACT1* was used as a loading control in Northern blots (D). *Pgk1* was used as loading control in Western blots (E). In strain A15615, we only examined *CLN2* RNA levels because chromosome XIV is not marked in this strain and we were therefore not able to select for the presence of two copies of this chromosome when introducing the Cln2-HA allele.

likely contribute to the phenotypes shared by aneuploids.

Striking among the phenotypes shared by aneuploid yeast strains are those indicative of protein degradation and folding distress. These observations suggest that proteins synthesized from the additional chromosomes disrupt cellular physiology, interfering with metabolic pathways and other basic cellular processes. We propose that the cell responds to this state of imbalance in a multilayered fashion not dissimilar to that of a stress response. The cell's attempt to restore wild-type physiology is reflected by the fact that although most genes present on the additional chromosomes are transcribed, the amounts of

many proteins are not increased. The decrease in biomass produced per glucose molecule may be an indicator that more energy is being used to degrade proteins and induce mechanisms that shield the cell from the effects of excess proteins or compensate for their effects. Even the delay in G_1 might be a reflection of basic cellular pathways (such as growth) being slowed down.

Cancer cells, most of which are aneuploid, share several properties with yeast cells carrying additional chromosomes. Proliferation of both types of cells is impaired in the presence of protein synthesis inhibitors (27) and geldanamycin (28), and both exhibit increased glucose

uptake (29). These parallels between tumor cells and aneuploid yeast strains raise the possibility that some phenotypes exhibited by tumor cells are elicited by their aneuploid state. Thus, the phenotypes exhibited by aneuploid yeast strains could be the starting point to determine whether aneuploid mammalian cells also share a set of phenotypes. These shared properties would be ideal targets for chemotherapeutics.

Our analysis shows that aneuploidy causes a proliferative disadvantage in yeast. The same could be true in human cells, not only because of the high degree of conservation of basic cellular processes among eukaryotes but also because trisomy 21 foreskin fibroblasts proliferate more

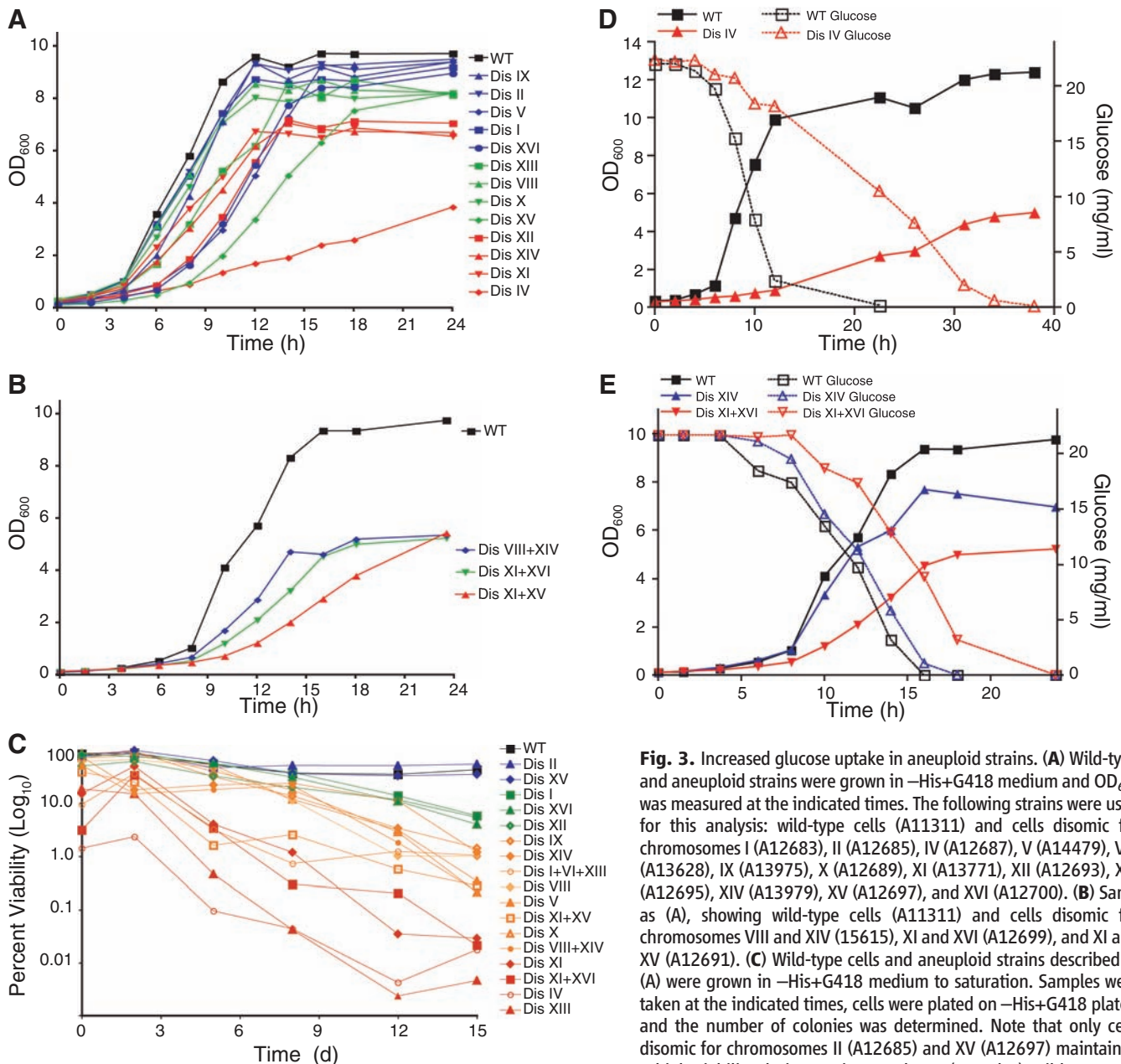


Fig. 3. Increased glucose uptake in aneuploid strains. (A) Wild-type and aneuploid strains were grown in $-His+G418$ medium and OD_{600} was measured at the indicated times. The following strains were used for this analysis: wild-type cells (A11311) and cells disomic for chromosomes I (A12683), II (A12685), IV (A12687), V (A14479), VIII (A13628), IX (A13975), X (A12689), XI (A13771), XII (A12693), XIII (A12695), XIV (A13979), XV (A12697), and XVI (A12700). **(B)** Same as (A), showing wild-type cells (A11311) and cells disomic for chromosomes VIII and XIV (15615), XI and XVI (A12699), and XI and XV (A12691). **(C)** Wild-type cells and aneuploid strains described in (A) were grown in $-His+G418$ medium to saturation. Samples were taken at the indicated times, cells were plated on $-His+G418$ plates, and the number of colonies was determined. Note that only cells disomic for chromosomes II (A12685) and XV (A12697) maintained a high viability during stationary phase. **(D and E)** Wild-type cells and cells disomic for chromosome IV (A12687) were grown to log phase and diluted into fresh medium, and the OD_{600} and amount of glucose in the medium were determined at the indicated times. **(E)** Same as (D) for wild-type cells and cells disomic for chromosome XIV (A13979) or XI+XVI (A12699).

and cells disomic for chromosome IV (A12687) were grown to log phase and diluted into fresh medium, and the OD_{600} and amount of glucose in the medium were determined at the indicated times. **(E)** Same as (D) for wild-type cells and cells disomic for chromosome XIV (A13979) or XI+XVI (A12699).

slowly than normal diploid fibroblasts (7). Is it thus possible that aneuploidy does not contribute to carcinogenesis but rather antagonizes it? Aneuploidy provides a means of gaining additional copies of oncogenes or losing tumor suppressor genes (4, 30), and the cellular imbalances caused by aneuploidy could create a selective stress that could promote the accumulation of growth and

proliferation-promoting genomic alteration. Under selective conditions, even in yeast, certain aneuploidies may be advantageous (31). However, our data show that aneuploidy in itself results in a proliferative disadvantage for the cell. Clearly, this disadvantage must be overcome during tumor formation through the acquisition of mutations that allow cells to tolerate aneu-

ploidy. The aneuploid yeast strains described here could provide the opportunity to identify such genes.

References and Notes

1. L. H. Hartwell, S. K. Dutcher, J. S. Wood, B. Garvik, *Rec. Adv. Yeast Mol. Biol.* **1**, 28 (1982).
2. M. J. Rosenstraus, L. A. Chasin, *Genetics* **90**, 735 (1978).

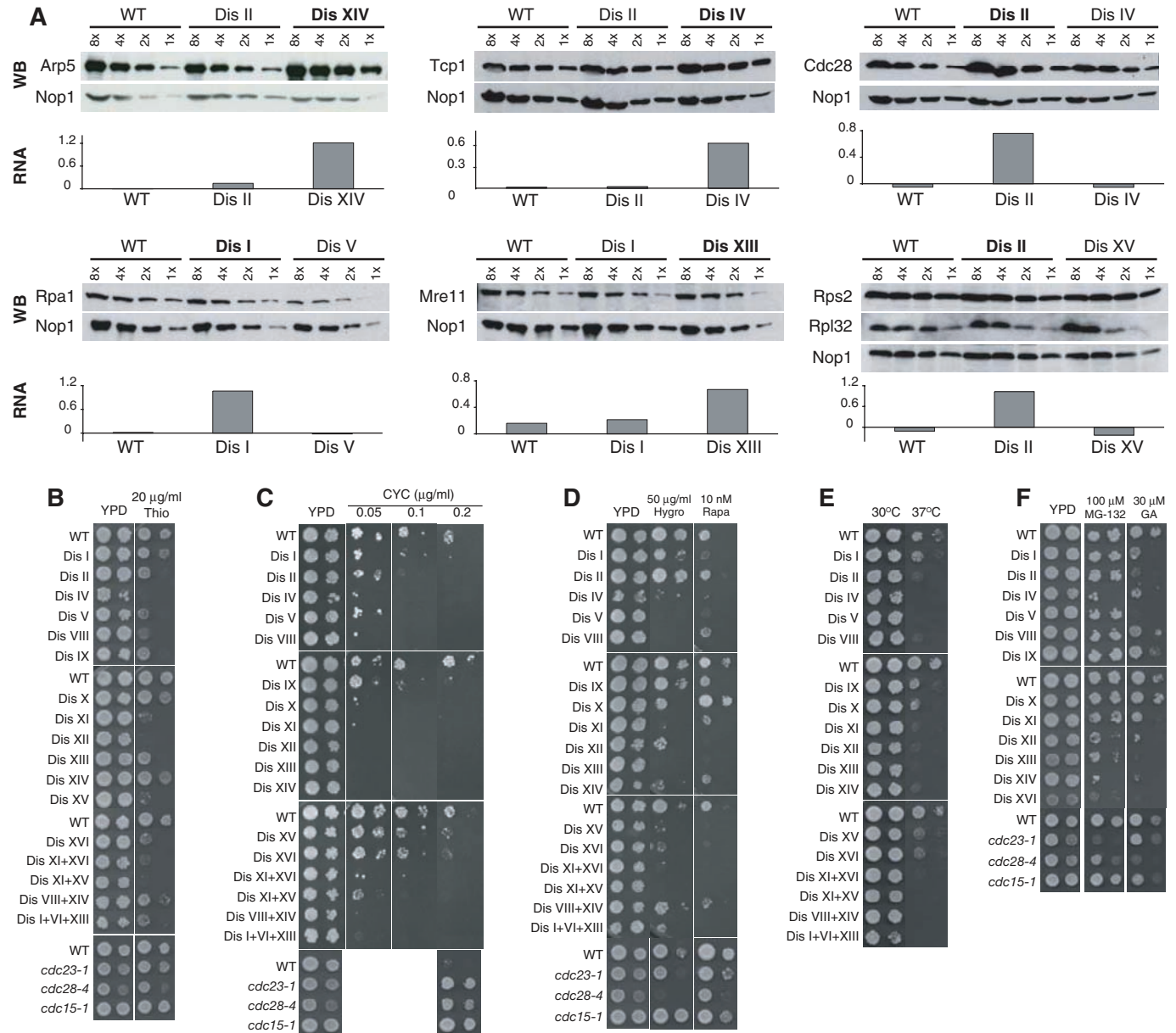


Fig. 4. Increased sensitivity of aneuploid strains to conditions interfering with protein synthesis and folding. (A) Examples of effects of increased gene dosage on protein abundance. Arp5, Tcp1, Cdc28, Rpa1, Mre11, Rps2, and Rpl32 proteins were examined in wild-type cells; in cells disomic for the chromosome on which the encoding gene is located; and in cells disomic for a different chromosome by Western blot analysis. Boldface type indicates the disome on which the encoding gene of interest is located. RNA levels of the gene product of interest are shown as a \log_2 ratio of wild type of an average of two microarray analyses below the blot. Nop1 was used as a loading control; 50 μg (8x), 25 μg (4x), 13 μg (2x), and 6 μg (1x) of extract were loaded. Arp5 protein and RNA levels were analyzed in wild-type (WT) (A11311), Dis II (A12685), and Dis XIV (A13979); Tcp1 in WT (A11311), Dis II (A12685), and

Dis IV (A12687); Cdc28 in WT (A11311), Dis II (A12685), and Dis IV (A12687); Rpa1 in WT (A11311), Dis I (A12683), and Dis V (14479); Mre11 in WT (A11311), Dis I (A12683), and Dis XIII (A12695); and Rps2 and Rpl32 in WT (A11311), Dis II (A12685), and Dis XV (A12697). (B to F) Proliferative capability of disomes in the presence of thiolutin (B), cycloheximide (C), hygromycin and rapamycin (D), high temperature (37°C) (E), and MG132 and geldanamycin (F); 10-fold dilutions are shown. Strains (from the top): A11311, A12683, A12685, A12687, A14479, A13628, A13975, A12689, A13771, A12693, A12695, A13979, A12697, A12700, A12699, A12691, A15615, A15614, A11311, A755, A2594, and A2595. In (F), the order is A15548, A15550, A15552, A15554, A15556, A15558, A15560, A15562, A15564, A15566, A15567, A15568, A15572, A11311, A755, A2594, and A2595.

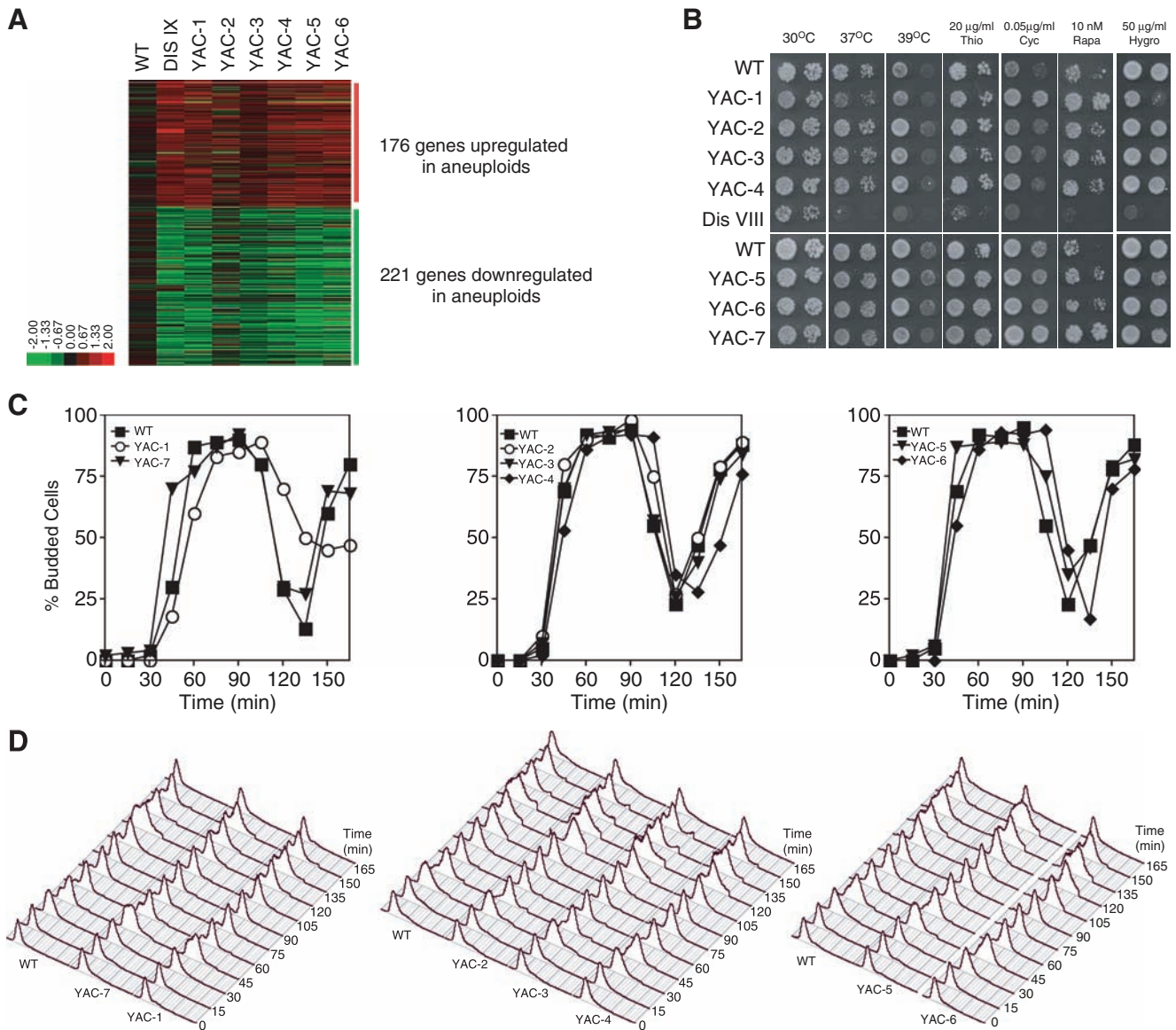


Fig. 5. Effects of human and mouse DNA on yeast. **(A)** Gene expression of YAC-containing strains grown under phosphate-limiting conditions. The gene expression pattern is shown for the 397 genes identified as changed in aneuploid strains grown under phosphate-limiting conditions. Genes increasing in expression in the aneuploid strains are marked by the red bar, and genes decreasing in expression by the green bar. Data for wild-type cells and cells disomic for chromosome IX are from Fig. 1C and are shown for comparison. Data are provided in table S5. Order of strains (from the left): A11311, A13975, A16854 (this strain contains a truncated version of YAC-1), A17392, A17393,

A17394, A17397, A16851. **(B)** Behavior of YAC-carrying strains and aneuploid strains in the presence of high temperature (37°C, 39°C), thiolutin, cycloheximide, rapamycin, and hygromycin. Strains (from the top): A11311, A16850, A17392, A17393, A17394, A13628, A11311, A17396, A17397, and A16851. **(C and D)** Wild-type cells (A11311) and cells carrying YAC-1 (A16850), YAC-7 (A16851), YAC-2 (A17392), YAC-3 (A17393), YAC-4 (A17394), YAC-5 (A17396), or YAC-6 (A17397) were released from a pheromone-induced G_1 arrest as described in Fig. 2. At the indicated times, samples were taken to determine the percentage of budded cells (C) and DNA content (D).

3. T. Boveri, *Neu Folge* **35**, 67 (1902).
4. C. Lengauer, K. W. Kinzler, B. Vogelstein, *Nature* **396**, 643 (1998).
5. O. Niwa, Y. Tange, A. Kurabayashi, *Yeast* **23**, 937 (2006).
6. D. L. Lindley *et al.*, *Genetics* **71**, 157 (1972).
7. D. J. Segal, E. E. McCoy, *J. Cell. Physiol.* **83**, 85 (1974).
8. J. Conde, G. R. Fink, *Proc. Natl. Acad. Sci. U.S.A.* **73**, 3651 (1976).
9. T. Nilsson-Tillgren, J. G. Litske, S. Holmberg, M. C. Kielland-Brandt, *Carlsberg Res. Commun.* **45**, 113 (1980).
10. See supporting material on Science Online.
11. T. R. Hughes *et al.*, *Nat. Biotechnol.* **19**, 342 (2001).
12. A. P. Gasch *et al.*, *Mol. Biol. Cell* **11**, 4241 (2000).
13. B. Regenberg *et al.*, *Genome Biol.* **7**, R107 (2006).
14. E. I. Boyle *et al.*, *Bioinformatics* **20**, 3710 (2004).
15. M. Costanzo *et al.*, *Cell* **117**, 899 (2004).
16. R. A. de Bruin, W. H. McDonald, T. I. Kalashnikova, J. Yates 3rd, C. Wittenberg, *Cell* **117**, 887 (2004).
17. C. Wittenberg, K. Sugimoto, S. I. Reed, *Cell* **62**, 225 (1990).
18. L. Dirick, T. Bohm, K. Nasmyth, *EMBO J.* **14**, 4803 (1995).
19. D. Stuart, C. Wittenberg, *Genes Dev.* **9**, 2780 (1995).
20. A. L. Lehninger, D. L. Nelson, M. M. Cox, *Principles of Biochemistry* (Worth, New York, ed. 2, 1993).
21. U. Schubert *et al.*, *Nature* **404**, 770 (2000).
22. E. Balzi, M. Wang, S. Leterme, L. Van Dyck, A. Goffeau, *J. Biol. Chem.* **269**, 2206 (1994).
23. P. H. Bissinger, K. Kuchler, *J. Biol. Chem.* **269**, 4180 (1994).
24. J. Hanna, D. S. Leggett, D. Finley, *Mol. Cell. Biol.* **23**, 9251 (2003).
25. W. Katz, B. Weinstein, F. Solomon, *Mol. Cell. Biol.* **10**, 5286 (1990).
26. A. Gunjan, A. Verreault, *Cell* **115**, 537 (2003).
27. J. B. Easton, P. J. Houghton, *Oncogene* **25**, 6436 (2006).
28. L. Whitesell, S. L. Lindquist, *Nat. Rev. Cancer* **5**, 761 (2005).
29. R. A. Gatenby, R. J. Gillies, *Nat. Rev. Cancer* **4**, 891 (2004).
30. B. A. Weaver, D. W. Cleveland, *Curr. Opin. Cell Biol.* **18**, 658 (2006).
31. M. J. Dunham *et al.*, *Proc. Natl. Acad. Sci. U.S.A.* **99**, 16144 (2002).
32. We thank D. Koshland, B. Brewer, J. Warner, and B. Adamson for reagents; C. Huttenhower, M. Hibbs, and O. Troyanskaya for use of the WCluster program; C. DeSevo for technical assistance; and D. Pellman, A. Hochwagen, F. Solomon, and members of the Amon

lab for suggestions and critical reading of this manuscript. A.A. thanks I. Hershkovitz for encouragement. Supported by NIH grant GM56800 and a David Koch Research Award (A.A.) and NIH grant GM071508 to the Lewis-Sigler Institute. A.A. is an Investigator of the Howard Hughes Medical Institute. All microarray data are available in final processed form in

table S5, and as raw data through the Princeton University MicroArray Database (puma.princeton.edu) and the Gene Expression Omnibus (GEO, www.ncbi.nlm.nih.gov/geo) under accession number GSE7812.

Materials and Methods
Figs. S1 to S8
References

Supporting Online Material
www.sciencemag.org/cgi/content/full/317/5840/916/DC1

7 March 2007; accepted 19 June 2007
10.1126/science.1142210

REPORTS

Detection of Circumstellar Material in a Normal Type Ia Supernova

F. Patat,^{1*} P. Chandra,² R. Chevalier,² S. Justham,³ Ph. Podsiadlowski,³ C. Wolf,³ A. Gal-Yam,⁴ L. Pasquini,¹ I. A. Crawford,⁵ P. A. Mazzali,^{6,7} A. W. A. Pauldrach,⁸ K. Nomoto,⁹ S. Benetti,¹⁰ E. Cappellaro,^{6,11} N. Elias-Rosa,^{6,11} W. Hillebrandt,⁶ D. C. Leonard,¹² A. Pastorello,¹³ A. Renzini,¹⁰ F. Sabbadin,¹⁰ J. D. Simon,⁴ M. Turatto¹⁰

Type Ia supernovae are important cosmological distance indicators. Each of these bright supernovae supposedly results from the thermonuclear explosion of a white dwarf star that, after accreting material from a companion star, exceeds some mass limit, but the true nature of the progenitor star system remains controversial. Here we report the spectroscopic detection of circumstellar material in a normal type Ia supernova explosion. The expansion velocities, densities, and dimensions of the circumstellar envelope indicate that this material was ejected from the progenitor system. In particular, the relatively low expansion velocities suggest that the white dwarf was accreting material from a companion star that was in the red-giant phase at the time of the explosion.

As a result of their extreme luminosities and high homogeneity, type Ia supernovae (SNe Ia) have been used extensively as cosmological reference beacons to trace the evolution of the universe (1, 2). However, despite recent progress, the nature of the progenitor stars and the physics that govern these powerful explosions remain poorly understood (3, 4). In the presently favored single-degenerate model, the supernova (SN) progenitor is a white dwarf that accretes material from a nondegener-

ate companion star in a close binary system (5); when it approaches the Chandrasekhar limit, the white dwarf explodes in a thermonuclear blast. A direct method for investigating the nature of the progenitor systems of SNe Ia is to search for signatures of the material transferred to the ac-

creting white dwarf in the circumstellar material (CSM). Previous attempts have aimed at detecting the radiation that would arise from the interaction between the fast-moving SN ejecta and the slow-moving CSM in the form of narrow emission lines (6), radio emission (7), and x-ray emission (8). The most stringent upper limit to the mass-loss rate set by radio observations is as low as 3×10^{-8} solar masses per year ($M_{\odot} \text{ year}^{-1}$) for an assumed wind velocity of 10 km s^{-1} (7). Two notable exceptions are represented by two peculiar SNe Ia, SN 2002ic and SN 2005gj, which have shown extremely pronounced hydrogen emission lines (9, 10) that have been interpreted as a sign of strong ejecta-CSM interaction (11). However, the classification of these supernovae as SNe Ia has recently been questioned (12), and even if they were SNe Ia, these supernovae are unlikely to account for normal SNe Ia explosions (7) that, of those observed so far, lack any signature of mass transfer from a hypothetical donor. Here we report direct evidence of CSM in a SN Ia that has shown normal behavior at x-ray, optical, and radio wavelengths.

SN 2006X was discovered in the Virgo cluster spiral galaxy NGC 4321 (13). A few days

¹European Southern Observatory (ESO), Karl Schwarzschild Strasse 2, 85748, Garching bei München, Germany. ²University of Virginia, Department of Astronomy, Post Office Box 400325, Charlottesville, VA 22904, USA. ³Department of Astrophysics, University of Oxford, Oxford OX1 3RH, UK. ⁴Astronomy Department, MS 105-24, California Institute of Technology, Pasadena, CA 91125, USA. ⁵School of Earth Sciences, Birkbeck College London, Malet Street, London WC1E 7HX, UK. ⁶Max-Planck-Institut für Astrophysik, Karl Schwarzschild Strasse 1, 85748, Garching bei München, Germany. ⁷Istituto Nazionale di Astrofisica (INAF)—Osservatorio Astronomico, via Tiepolo 11, 34131 Trieste, Italy. ⁸Institut für Astronomie und Astrophysik der Ludwig-Maximilians-Universität, 81679 Munich, Germany. ⁹Department of Astronomy, University of Tokyo, Bunkyo-ku, Tokyo 113-0033, Japan. ¹⁰INAF—Osservatorio Astronomico, vicolo Osservatorio 5, 35122 Padova, Italy. ¹¹Universidad de La Laguna, Avenida Astrofísico Francisco Sánchez s/n, E-38206, La Laguna, Tenerife, Spain. ¹²Department of Astronomy, San Diego State University, San Diego, CA 92182, USA. ¹³Astrophysics Research Centre, Queen's University Belfast, BT7 1NN, UK.

*To whom correspondence should be addressed. E-mail: fpatat@eso.org

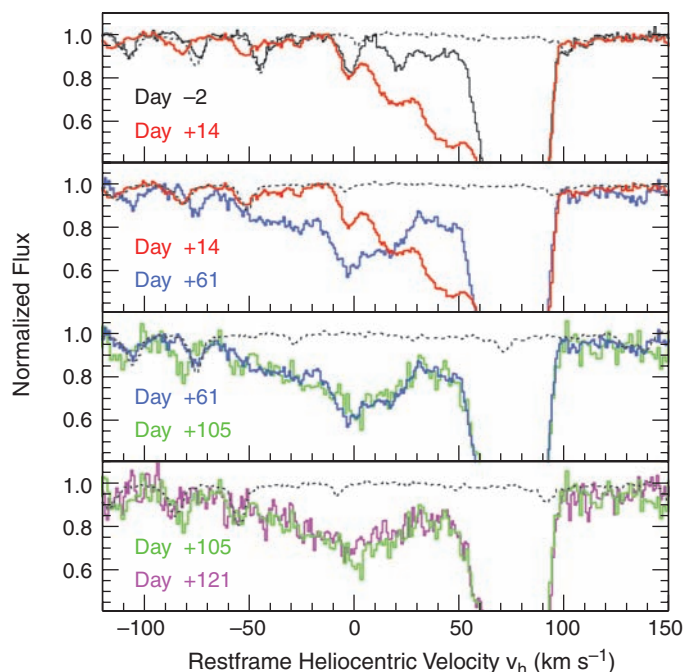


Fig. 1. Time evolution of the Na D₂ component region as a function of elapsed time since B-band maximum light. We corrected the heliocentric velocities to the rest-frame using the host galaxy recession velocity. All spectra have been normalized to their continuum. In each panel, the dotted curve traces the atmospheric absorption spectrum.